



## Contribution of Southern Indian Ocean swells on the wave heights in the Northern Indian Ocean—A modeling study

L. Sabique\*, K. Annapurnaiah, T.M. Balakrishnan Nair, K. Srinivas

Indian National Centre for Ocean Information Services (INCOIS), P.B. No. 21, Jeedimetla-IDA P.O., Hyderabad-500 055, India

### ARTICLE INFO

#### Article history:

Received 2 June 2011

Accepted 29 December 2011

Editor-in-Chief: A.I. Incecik

#### Keywords:

Wave modeling

Indian Ocean

Wave validation

Swell propagation

### ABSTRACT

Waves are important driving forces that have important ramifications for physics, chemistry and biology of the coastal and open ocean. An attempt is made to study the swell propagation from Southern Indian Ocean and to account for its contribution to the local wave climate in Northern Indian Ocean. The third generation ocean wave model, MIKE 21 SW is implemented and validated to simulate wave heights for the period starting from September 2008 to August 2009 for the Indian seas. Simulations were carried out by modifying the analyzed winds over the model domain (30°E–120°E and 60°S–30°N). It was found that Southern Indian Ocean swells play an important role in determining the Northern Indian Ocean wave climate. Under the influence of the southwest summer monsoon winds, the swell dominance on the local wave climate drops in the Bay of Bengal but not as much as in the Arabian Sea due to the strong and persistent southwest winds during the summer monsoon. During the rest of the year, the swell is a dominant factor in determining the wave climate of the Northern Indian Ocean.

© 2012 Elsevier Ltd. All rights reserved.

### 1. Introduction

Knowledge of the contribution of ocean swell to the local wave climate is of great importance for wide range applications: coastal oceanographic studies, coastal management activities and ocean engineering. Every coastal or ocean engineering project such as a oil rig or harbor designing, requires the information of wave conditions in the region of interest. Thus, the primary coastal oceanographic parameter of concern for the coastal engineer project is the wave climate at the site and the resultant forces on the moored tankers and structures associated with the berth. Usually, wave characteristics are collected offshore and it is necessary to extrapolate these offshore data on wave heights and wave propagation direction to the project site. In the early 1960s, the wave ray tracing method was a common tool for estimating wave characteristics at a design site. Today, powerful computers have provided coastal engineers with the opportunity to employ more sophisticated numerical models for wave environment assessment. Swells are today the most poorly predicted part of the sea state, with detrimental impact on delicate marine operations because of its high energy compared to the locally generated wind seas. In the present study, an attempt is made to study the propagation pattern and quantify the Southern Indian

Ocean swell contribution in the wave climate over the Northern Indian Ocean.

Satellite data show that there are three well-defined swell dominant zones in the tropical areas of Pacific, Atlantic and Indian Oceans. The persistent, strong, winds over the southern oceans generate high waves that travel thousands of kilometers to the Indian Ocean as large swell component (Alves, 2006). These swells on entering the Indian Ocean region, contribute to the total wave height of the surface waves. Studies on swells and their propagation have been of great interest to many researchers over the decades. Munk (1947) made an attempt to track the storms by using forerunners of the swells. Barber and Ursell (1948) measured frequency spectra of ocean waves in order to develop a reliable method of predicting amplitude and period of wind waves and swell from meteorological charts and forecasts. Snodgrass et al. (1966) focused on the evolution of the swell energy along the propagation direction in North Atlantic Ocean. These early works provided important insights on swell generation and propagation that have stood the proof of time, and are still valid paradigms today. Studies conducted over the last few decades have expanded these initial insights, revealing that the presence of swell affects several important processes at the air–sea interface, such as the modulation, blockage and suppression of short period wind-generated waves. Hanson and Phillips (1999) investigated the wind sea growth and dissipation in a swell-dominated, open ocean environment to explore the use of wave parameters in air–sea process modeling. An automated

\* Corresponding author. Tel.: +91 40 23895017; fax: +91 40 23892910.  
E-mail address: [sabique.l@gmail.com](mailto:sabique.l@gmail.com) (L. Sabique).

swell tracking and storm identification system was developed using the wave portioning method (Hanson and Phillips, 2001). Ardhuin et al. (2009) provided an accurate estimation of the dissipation rates of swell energy across the oceans. Finally, Ardhuin et al. (2010) proposed a set of parameterization for the dissipation source terms of the wave energy balance equation, based on known properties of swell dissipation and wave breaking statistics. All these studies essentially followed swells along a great circle and showed that it was possible to estimate swell heights fairly accurately.

The annual wind patterns for north Indian Ocean can be divided into four seasons: (i) northeast monsoon: December–March (henceforth D–J–F–M); (ii) pre-monsoon season: April–May (henceforth A–M); (iii) southwest monsoon: June–September (henceforth J–J–A–S) and (iv) post-monsoon season: October–November (henceforth O–N). Hence the wave climate over this region is unique in the world ocean. There are many previous studies which describe the wind and wave climate in the Northern Indian Ocean. Wind speeds over Indian Ocean increase during mid May and high winds are observed up to September, which is the period of the summer monsoon. Along the west coast of India, significant wave height up to 6 m is reported during the summer monsoon period (Kumar, 2006) whereas the significant wave height will be normally less than 1.5 m during rest of the year (Kumar and Anand, 2004). Young (1999) concluded that the Indian Ocean basin is strongly affected by the Southern Indian Ocean swell, especially during the Southern Hemisphere winter (i.e., June–September) based on a study using merged global wave climatology derived from satellite observations and models. The wave characteristics in the Indian Ocean region have been studied by different researchers by using models and observational data. Vethamony et al. (2006) and Sudheesh et al. (2004) used MIKE 21 OSW model to generate the offshore waves by using NCMRWF winds. Recently, Aboobacker et al. (2011a,b) estimated dominance of swells and wind seas on monthly and seasonal basis along the west coast of India and Vethamony et al. (2011) studied the superimposition of locally generated waves from Northwest with the pre-existing swell from Southwest in the off Goa, west coast of India. Further, Bhowmick et al. (2011) investigated the

propagation patterns of the swells over Indian Ocean by long term simulation of significant wave heights for 13 years using spectral ocean wave model (WAM). The propagation of “Shamal” swells and their influence along the west coast of India are studied by Aboobacker et al. (2011a,b). All these earlier works emphasize the fact that, for accurate wave prediction over the Indian Ocean, swell part of the waves should be critically taken into account. However, to date there has been little or no study on the contribution of Southern Indian Ocean swell to the wave climate over Northern Indian Ocean.

To evaluate the generation and propagation of swells in intense storm areas, a numerical wave modeling technique was developed by modifying the wind fields (Alves, 2006). In this present study, we have adapted the discretisation technique proposed by Alves (2006) with minor modifications. Simulations were conducted with the help of numerical models to generate wind sea areas, and these areas are isolated from the adjacent regions of the model domain, where surface winds are almost switched off but swells are allowed to propagate freely. In the first simulation (henceforth S1), the calibrated and validated wave model is run with real forcing fields all over the model domain. In the second simulation (henceforth S2), the same model used for S1 is forced with real wind fields over the swell generating areas of the Southern Indian Ocean (60°S–40°S) only, and the speeds of the wind fields over rest of the model domain is reduced to zero, so that the wave generated over Southern Indian Ocean (expected as swells) are propagated towards the Northern Indian Ocean freely. The study domain and the area where the forcing is given are shown in the Fig. 1.

## 2. Data used

### 2.1. Wind forcing for the model

The sensitivity of waves to the quality of winds was confirmed by Janssen (1998), who showed that random wind speed errors dominate the forecast wave height errors even after the 48 h-forecast. Further, it has been shown that in the tropics, where sea

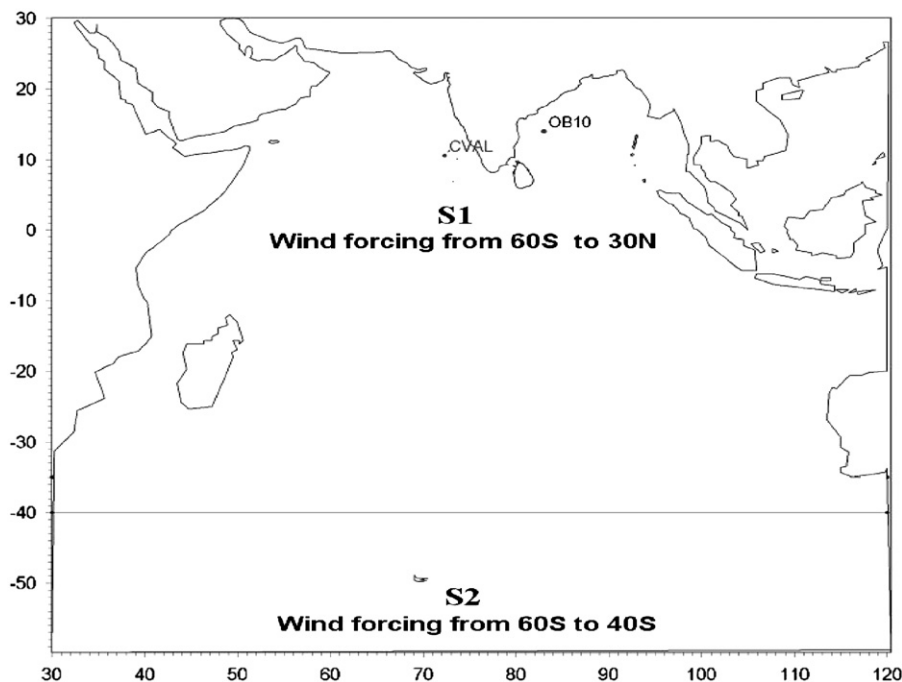


Fig. 1. Study area with zones showing areas of modification of wind. The buoys (CVAL and OB10) used for validation are also shown.

state is dominated by swell, quality of wave model outputs depend on the quality of the wind field in the extra tropics where swells are generated (Janssen, 2000). Wave models are thus extremely sensitive to details of the input wind and a high quality winds only reproduce the real wave climate. A high quality analyzed surface wind field provided by National Center for Medium Range Weather Forecast (NCMRWF) was used in the present study. The NCMRWF uses T254L64 spectrum model that utilizes all conventional and non-conventional data received through Global Telecommunication System (GTS) at Regional Telecommunication Hub (RTH), New Delhi. Non-conventional data include cloud motion vectors (CMVs) from INSAT, GMS, GOES and METEOSAT satellites, NOAA satellite temperature profiles and three layer precipitable water content, surface wind information from ERS-2 satellite, etc. (Parrish et al., 1997; Rizvi et al., 2000). The six hourly surface wind fields, with spatial resolution of  $0.5^\circ \times 0.5^\circ$  derived from T254L64 model for the period starting from September 2008 to August 2009 was used to simulate the waves over Indian Ocean.

## 2.2. Buoy data

In the Indian Ocean region, several deep-sea and shallow water moored buoys have been deployed by the National Institute of Ocean Technology, Chennai since 1997 (Premkumar et al., 2000) under the National Data Buoy Program (NDBP) measure several near surface meteorological and oceanic variables. The buoy data have proved to be extremely useful in validating re-analysis and satellite products (Sengupta et al., 2001; Senan et al., 2001). The buoy data consists of wind speed and direction at every 3 h intervals. Each three-hourly wind observation is a 10 min average wind speed and direction sampled at 1 Hz by a cup anemometer with vane installed at 3 m height above the sea level. The accuracy of wind speed measurements is 1.5% of full scale ( $0\text{--}60 \text{ ms}^{-1}$ ), i.e.,  $0.9 \text{ ms}^{-1}$ .

The sensor used in the measurement of wave parameters is an inertial altitude heading reference system with dynamic linear motion measurement capability. The waves are measured in the buoy by a motion reference unit, which measures absolute roll, pitch, yaw and relative heave. These data are recorded at a rate of 1 Hz for 17 min every three hours. The SWH is estimated as four times the square root of the area under the non-directional wave spectrum.

The geographical coverage of the buoy data is very limited, and no buoy has functioned continuously. Hence, buoys having continuous observations of more than two months duration for the simulation period is only considered for comparison. Based on the length of data available with minimum gaps during the period 2008–2009, two buoy—one in the AS (CVAL, Lat:  $10.61^\circ\text{N}$ , Lon:  $72.29^\circ\text{E}$ ) and one in the BOB (OB10, Lat:  $14^\circ\text{N}$ , Lon:  $83^\circ\text{E}$ ) were selected for the present study and the buoy locations are shown in Fig. 1. Further, the wave parameters for the CVAL location are not available for the study period.

## 3. MIKE 21 spectral wave model

MIKE 21 Spectral Wave (MIKE 21 SW) model is one of the state-of-the-art numerical modeling tools for studying spectral wind-wave modeling. The model is based on flexible mesh and therefore is particularly applicable for simultaneous wave analysis both on regional and local scales. Flexible mesh allows for coarse spatial resolution for offshore area and high-resolution mesh in shallow water near the coastline. The model simulates wave growth by the action of wind, non-linear wave-wave interaction, dissipation due to white-capping, bottom friction

and depth-induced wave breaking, refraction and shoaling due to depth variations, wave-current interaction and effect of time-varying water depth. The model is based on numerical integration of energy balance equation formulated in Cartesian co-ordinates.

$$\mathbf{DE}/\mathbf{Dt} = \mathbf{S}_{\text{wind}} + \mathbf{S}_{\text{nonlinear}} + \mathbf{S}_{\text{bottom-dissipation}} + \mathbf{S}_{\text{white-capping}} + \mathbf{S}_{\text{wave-breaking}}$$

The LHS describes the wave spectral energy ( $E$ ) propagation in space and time and the RHS represents the superposition of source functions describing various physical phenomena. MIKE21 SW model is appropriate for both off-shore and near-shore wave modeling as it includes two different formulations: (a) directional decoupled parametric formulation and (b) fully spectral formulation. The first formulation is suitable for near shore and the second one is more suitable for off-shore spectral wave modeling (DHI Manual, 2009). In this study, the second formulation has been used, as the study area is mainly located offshore. For the fully spectral formulation, the wind input source term is parameterized following Janssen's formulation and implemented as in WAM cycle 4 (Komen et al., 1994).

The standard application of white capping over the entire spectrum may result in too strong decay of energy on the swell components especially in the areas where combination of wind-sea and swell exist. Hence, MIKE 21 SW introduce a separation of wind-sea and swell, the predictions for these cases can be improved by excluding the dissipation on the swell part of the spectrum and by calculating the wave parameters, used in the formulation of white capping, from the wind-sea part of the spectrum. As a standard, the mean frequency, used in the determination of the maximum prognostic frequency is also calculated based on the whole spectrum. In the present study, dynamic threshold frequency is used for the separation of wind sea and swell.

## 4. Results and discussion

In this section, we will present the validation results obtained for the wind used for forcing the model, model simulated "wave" parameters and finally, the conclusions obtained from the experiments conducted for assessing the effect of Southern Indian Ocean swells on the wave climate over the Northern Indian Ocean. Various statistical measures—mean error (bias), root-mean-square error (RMSE), scatter-index (SI), and Pearson correlation coefficient ( $r$ ), are used to assess the quality of wind forcing and wave model performance by comparing with the corresponding buoy observations, computed as

$$\text{Bias} = \frac{1}{n} \sum (M_i - B_i) \quad (1)$$

$$\text{RMSE} = \frac{1}{n} \sqrt{\sum (M_i - B_i)^2} \quad (2)$$

$$\text{SI} = \frac{\text{RMSE}}{\bar{B}} \quad (3)$$

$$r = \frac{\sum (M_i - \bar{M})(B_i - \bar{B})}{\sqrt{\sum (B_i - \bar{B})^2} \sqrt{\sum (M_i - \bar{M})^2}} \quad (4)$$

where  $B_i$  and  $M_i$  indicate buoy measure and wind forcing/modeled wave parameters, respectively;  $\bar{B}$  and  $\bar{M}$  are their corresponding mean values and  $n$  is the number of observations used for the comparison.

Since the wind regimes and their corresponding wave regimes are different for different seasons as described in the introduction, the effect of the Southern Indian Ocean swells on Northern Indian Ocean wave climate is studied by analyzing the model simulations for separate seasons.

#### 4.1. Wind validation

The quality of the simulated wave height depends mainly on the accuracy of the wind fields used. The wave heights approximately scale with the square of wind speed and this implies that an error of about 10% in the driving wind fields will result in an error of at least 20% in the hind cast wave height (Pillar et al., 2008). To assess the quality of the wind forcing, an attempt is made to compare the NCMRWF analyzed winds with the observations from NDBP buoys. Since the buoy measurements of the wind speed are made at 3 m height, wind speed from the buoy ( $W_z$ ) were transformed to wind speeds at 10 m elevation ( $W_{10}$ ), using Prandtl 1/7 law approximation (Streeter et al., 1998) using the equation  $W_{10}/W_z = (10/z)^{1/7}$ . Here,  $z$  is the wind measurement height of the buoy which is 3 m. The comparison between NCMRWF and buoy data was performed for one location each in the Arabian Sea (CVAL), and Bay of Bengal (OB10), respectively. Natural neighbor interpolation method is used to interpolate gridded NCMRWF wind speed into individual buoy locations. This interpolation method is particularly effective for dealing with a variety of spatial data exhibiting clustered or highly linear distributions. The weights used in natural neighbor interpolation are based on amount of influence any scatter point will have on the computed value at the interpolation point. This amount of influence is entirely dependent on the area of influence of the of the surrounding scatter points to the interpolation point.

The NCMRWF wind speeds showed good agreement with buoy measured wind speeds in the Arabian Sea and Bay of Bengal as is evident in the time series plots (Fig. 2). From the time series plots, it is clear that the NCMRWF winds do not have appreciable bias with respect to observations at the buoy locations. The detailed statistics of the validation is presented in Table 1.

The average NCMRWF wind speed and standard deviations show the same range as buoy observations for both locations. However, standard deviation reveals that, the buoy measured wind speeds are more scattered as compared to NCMRWF winds. A correlation coefficient of 0.83 and 0.88 are obtained for CVAL and OB10, respectively. These high correlation coefficients suggest that, both NCMRWF and buoy measured winds follow a similar annual march. To determine the characteristics of the directional variability along with their magnitudes, the rose plots for both observation and wind forcing are drawn. Seasonal directional variability of winds along with their magnitudes is subtle and the same can be observed for almost all seasons from the rose plots (Fig. 3).

The rose plots reveal that the buoy measured seasonal distribution of the winds and their directional variability with respect to seasons are well represented in the NCMRWF model winds also. Further, the mismatches in the rose plot may be due to the model inefficiency in predicting the directions. The occurrence of the southwesterly waves is slightly underestimated by the NCMRWF winds. The high correlation together with low scatter index suggests that the NCMRWF wind is of good quality and can be used for the present study.

#### 4.2. Model validation

Validation of a model for a specific geographic location against observation is an important step involved in the development of

**Table 1**

The statistics of the comparison between buoy and NCMRWF wind speeds.

Buoy location	Average (m/s)		Standard deviation (m/s)		Bias (m/s)	RMSE (m/s)	Correlation
	Buoy	NCMRWF	Buoy	NCMRWF			
CVAL	8.01	6.76	5.03	4.49	-0.61	1.65	0.83
OB10	10.11	8.34	7.01	6.34	-0.63	1.7	0.88

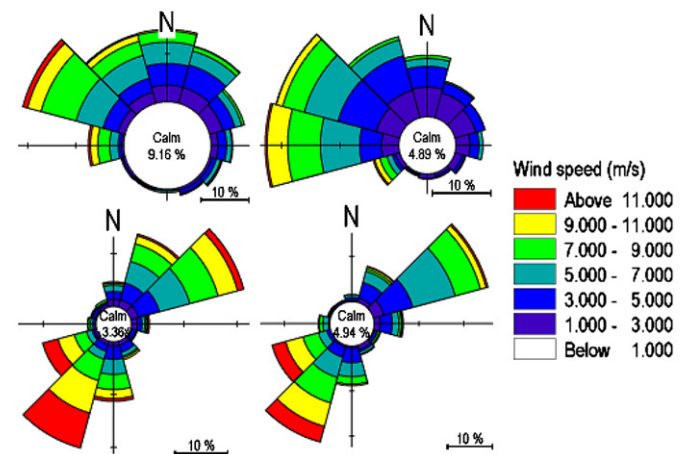


**Fig. 3.** Directional histograms of wind speeds, comparing measured (left) and modeled (right) data at buoy locations CVAL (above) and OB10 (below).

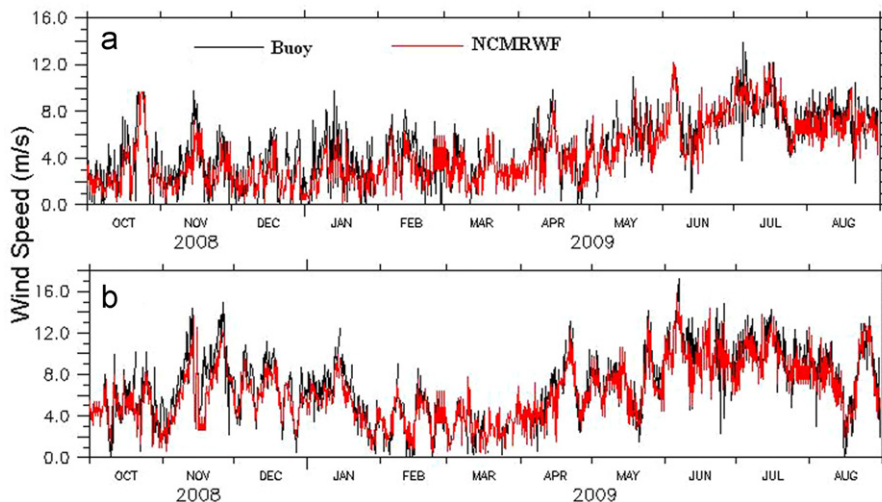


**Fig. 2.** Time series plots of buoy and NCMRWF wind speeds (a) at location CVAL and (b) OB10.

wave predictions and analysis (Khandekar, 1989). Based on the availability of buoy data in the study period, a comparison is made between buoy and model derived wave heights at one buoy location in Bay of Bengal (OB10) for October 2008 to August 2009. To evaluate the model performance, model simulated significant wave height, mean wave direction and mean wave period are compared with the buoy observations. The comparison shows that the model derived wave parameters agree well with the observed wave parameters as shown in Fig. 4. Qualitatively, the model output obtained here are consistent with those obtained at the buoy location. It is observed that the model could reproduce the lows as well as highs of the wave height at that buoy location. The simulated mean wave period shows a constant negative bias throughout the simulation period with a higher discrepancy in the March and April months. One conspicuous feature from the comparison of mean wave direction is that, the model could simulate the observed direction well irrespective of the seasons.

The detailed statistics of the validation is presented in Table 2. The model simulated wave parameters do not have much deviation from the observations. As observed in the winds, the buoy measured wave parameters are more scattered as compared to model simulated parameters. A general feature noticed from these results is that there is definite indication of different

performance of the model during the different seasons. The results are consistently better when the meteorological conditions are more defined and winds are stronger viz. southwest monsoon. The results degrade in the low wind conditions, especially in northeast monsoon, with severe underestimation of the wave heights indicating the poor performance of the model in low wind conditions. The reasons for the poor performance of the model in low wind conditions and fine tuning are beyond the scope of this paper. However, the overall performance, summarized by the statistics in Table 2, suggests the model performance is good.

The seasonal directional variability of waves along with their magnitudes can be assessed using the rose plots as shown in Fig. 5. The overall comparison shows similar wave patterns for both the measured and modeled data. It is observed that, 8.97% of the buoy measured wave heights are below 0.75 m; but only 3.32% represents less than 0.75 m waves in simulated waves. This gives an insight to the overestimation of the low wave heights in the model. Comparing the seasonal distribution of waves, during southwest monsoon the directions are very similar, with the main direction of incidence being from the southwest. The model slightly underestimates the occurrence of higher waves from the all directions and this underestimation is possibly linked with

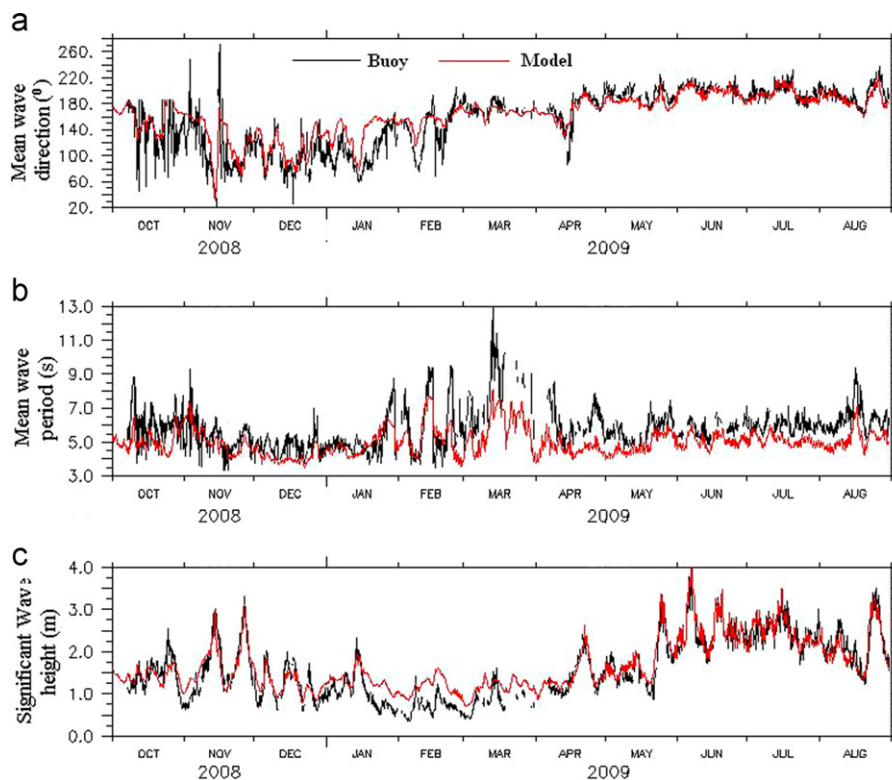


Fig. 4. Time series plots of buoy and model simulated wave parameters at location OB10 (a) Mean wave direction, (b) mean wave period and (c) significant wave height.

Table 2

The statistics of the comparison between buoy and simulated wave parameters.

Parameters	Average		Standard deviation		Bias	RMSE	Scatter index (%)	Correlation
	Buoy	Model	Buoy	Model				
Significant wave height (m)	1.58	1.68	0.50	0.51	0.11	0.30	19.0	0.93
Mean wave period (s)	5.83	5.00	1.48	0.76	-0.81	1.2	20.8	0.67

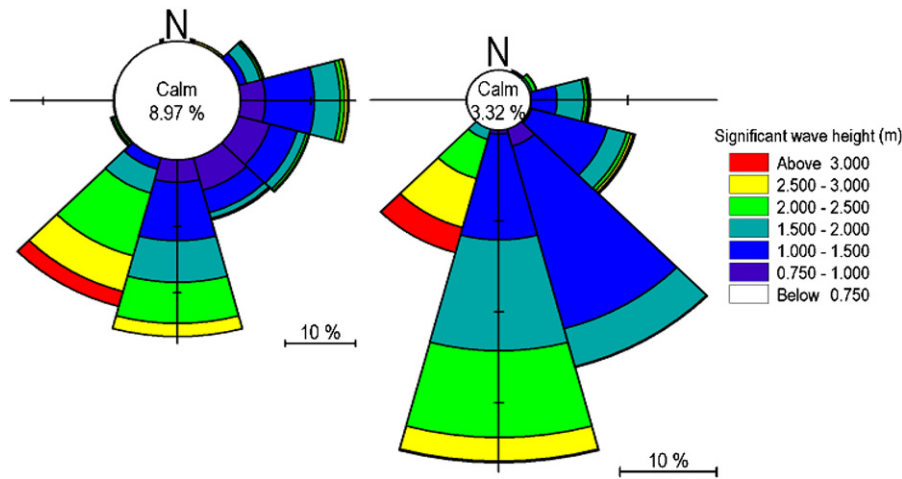


Fig. 5. Directional histograms of wave heights, comparing measured (left) and modeled (right) data at buoy location OB10.

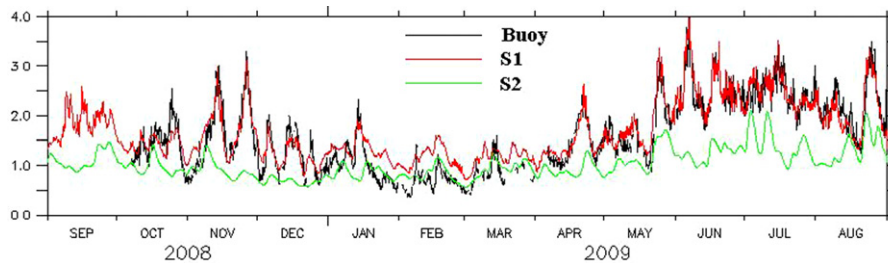


Fig. 6. comparison plots of simulated significant wave heights at location OB10 for S1 (red curve) and S2 (green curve) along with buoy measurements (black curve). (For interpretation of the references to color in this figure legend, the reader is referred to the web version of this article.)

the directional discrepancy linked with the wind forcing as seen in the directional histograms of the wind. Easterly waves are not well represented by the model, including the height classes. These comparisons, although qualitative, show that the overall wave climate is well represented by the model for the year compared at the buoy location OB10.

#### 4.3. Contribution of southern Indian Ocean swells on local wave climate

Two simulations were carried out using discretized wind fields as described in the introduction. The underlying model setup and bathymetry are kept the same for all simulations. For the Indian Ocean, typical swells of 7–10 s period traveling at speeds of  $10\text{--}15\text{ ms}^{-1}$  will cross the basin in 10 day or fewer (Kalantzi et al., 2009). A spin-up period of 15 day is given to each model run to ensure that all swell systems with long residence time are well captured so that the model results being analyzed are not affected by the initial conditions.

To estimate the Southern Indian Ocean swell contribution to the Northern Indian Ocean wave climate, the wave heights obtained from the two simulations S1 and S2 for a particular buoy location (OB10) in the Bay of Bengal along with buoy observation are shown in Fig. 7. There has been little or no evidence that swells influence wind sea growth, over the range of frequencies observed by wave buoys, in the open ocean (Hanson and Phillips, 2001) and at present there is no consensus on the plausible causes of the loss of swell energy [WISE Group, 2007]. Since swells can propagate freely without any influence of local winds, it is expected that the wave heights obtained in the S2 is the swell contribution to the local wave climate.

An average wave height of 1 m is observed irrespective of the season as a result of swell propagation from the Southern Indian Ocean (Fig. 6). The total wave climate in the northeast monsoon is largely affected by Southern Indian Ocean swells in both Arabian Sea and Bay of Bengal. As expected, there is an increased swell contribution in the austral winter (south-west monsoon), but the wind seas generated by the strong monsoon winds over the Northern Indian Ocean drives wave climate in that season.

The seasonally averaged wave heights from S1 and S2 are shown in Fig. 7. The results are as anticipated, as one would expect weaker ocean state over weaker wind areas. The results are in agreement with the seasons i.e., high wave conditions in strong wind seasons viz. southwest monsoon and low wave conditions in poor wind conditions. During the southwest monsoon season, large wave heights in the coastal region are a conspicuous feature, unlike the other seasons when the wave heights are smaller in the coastal regions. Maximum wave heights of the order of 5–7 m were noticed in the Southern Indian Ocean region for all seasons—in the region of Roaring Forties and Furious Fifties. Only during the southwest monsoon season, Northern Indian Ocean shows high wave heights of the order of 4–5 m in Somalia region and 3–4 m in the Bay of Bengal unlike other seasons.

The forcing in the Southern Indian Ocean generates swell systems that spread freely into large areas of the Southern and Northern Indian Ocean. The free propagation of these swell systems towards the north results in wave heights in the range of 1–1.5 m over Northern Indian Ocean. A conspicuous feature of Southern Indian Ocean swells is their east-northeastward propagation. As a result, the swells are propagating more into Bay of Bengal compared to Arabian Sea. Southern Indian Ocean swells also produce a significant signal in the higher latitudes of the

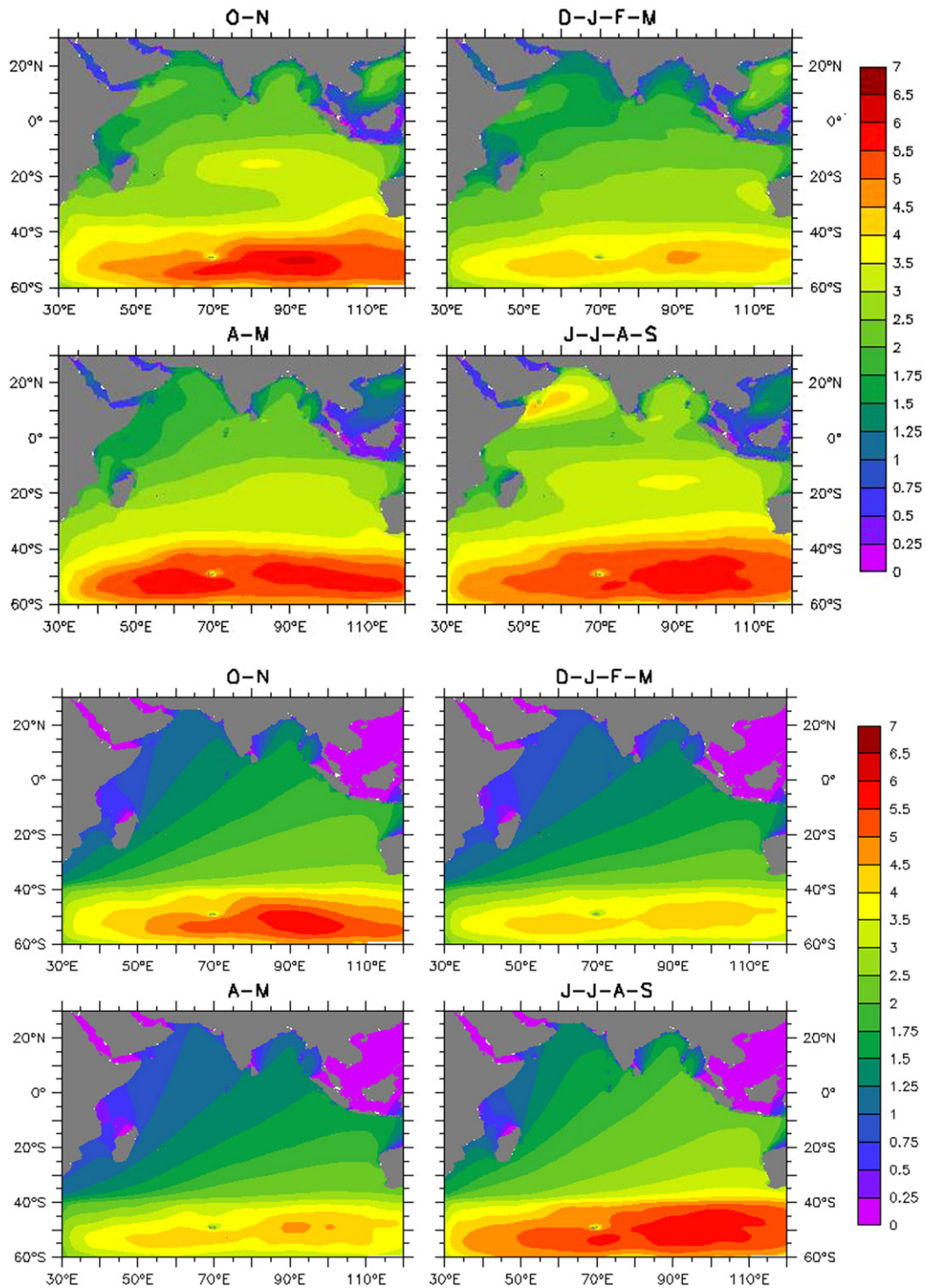


**Fig. 7.** The average simulated wave heights over the study domain during different seasons for S1 (above) and for S2 (below).

South Indian Ocean basin. Another noteworthy feature is that the Madagascar Island and Sri Lanka may be playing a role, although small in reducing the swell height along the western Arabian Sea and western Bay of Bengal by forming a shadow zone.

During O–N months, S2 shows a wave height of 0.5–1.5 m for the Northern Indian Ocean. A larger wave height of 4.5 m is propagated towards the north and it reduces to a value of 2.5–3.0 m near to the equator. For the months of D–J–F–M, the intensity of propagated waves is low compared to previous months which, in turn, reduce the extent of its effects over the

Northern Indian Ocean. The reduced wind speeds over the Southern Indian Ocean in the southern summer leads to this reduction. During A–M, the simulation shows wave heights of around 1–1.5 m in the Bay of Bengal and Arabian Sea. The large waves having 2–3 m is limited to 20° S. The extent of influence of Southern Indian Ocean swells is seen even beyond the equator; it even shows considerable effect in the Arabian Sea too. Finally, during the months of southwest monsoon (J–J–A–S), the S2 show maximum wave heights in the Northern Indian Ocean as compared to rest of the seasons. Waves having wave height greater

than 2.5 m cross the equator and freely propagate to the Arabian Sea and Bay of Bengal, where their heights are around 1.0–2.0 m.

On comparing the two simulations, the total waves (S1) and the swells (S2) from the Southern Indian Ocean, we found out a large influence of southern ocean swells in determining the wave climate over the Northern Indian Ocean. But the interaction with swells with locally generated wind waves can be better studied using wave spectra.

## 5. Conclusion

Swells are today the most poorly predicted part of the sea state, having a detrimental impact on some delicate marine operations. The third generation ocean wave model, MIKE 21 SW was successfully implemented and validated to provide wave hindcast for duration of one year starting from September, 2008 to August, 2009 for the Indian Ocean using NCMRWF, New Delhi analyzed wind speeds. An attempt was made to account for the contribution of swells from Southern Indian Ocean to Northern Indian Ocean by two simulations for significant wave heights in Indian Ocean with discretized wind fields; the first simulation with NCMRWF winds for the entire Indian Ocean (60°S–30°N) and second simulation with winds over 60°S–40°S region which allows swells generated in the Southern Indian Ocean were allowed to freely propagate into the Northern Indian Ocean. The comparison of two simulations would give idea about the contribution of Southern Indian Ocean swells in the Northern Indian Ocean. The second simulation showed northeastward propagation of swells from Southern Indian Ocean to Northern Indian Ocean during all seasons. The increased swell propagation from Southern Indian Ocean to Northern Indian Ocean during the months of June, July, August and September months can be attributed to the southern winter. In general, Bay of Bengal and Arabian Sea experience swell heights of 0.5–1.0 m, which are propagated from the Southern Indian Ocean. From the present study, it is clear that the swells represent a significant portion of wave heights in the Northern Indian Ocean and have more influence on the Bay of Bengal than the Arabian Sea. However, interaction between the swells and wind seas has to be investigated further to get a better understanding.

## Acknowledgment

This work is done as part of developing a wave forecasting system for India at Indian National Center for Ocean Information Services (INCOIS), India. Authors express sincere gratitude to Director, INCOIS, Hyderabad for encouragement and support. They are also thankful to National Data Buoy Program of National Institute of Ocean Technology, Chennai and Data Management Group of INCOIS for buoy data.

## References

Aboobacker, V.M., Rashmi, R., Vethamony, P., Menon, H.B., 2011a. On the dominance of pre-existing swells over wind seas along the west coast of India. *Cont. Shelf Research* 31, 1701–1712.

Aboobacker, V.M., Vethamony, P., Rashmi, R., 2011b. Shamal swells in the Arabian Sea and their influence along the west coast of India. *Geophysical Research Letters* 38 (3), 7 pp.

Alves, J.H.G.M., 2006. Numerical modeling of ocean swells contributions to the global wind-wave climate. *Ocean Modelling* 11, 98–122.

Ardhuin, F., Bertrand, C., Fabrice, C., 2009. Observation of swell dissipation across oceans. *Geophysical Research Letters* 39, 1–5.

Ardhuin, F., Rogers, E., Babanin, A.V., Filipot, J.F., Magne, R., Roland, A., Westhuysen, A., Queffelec, P., Lefevre, J.M., Aouf, L., Collard, F., 2010. Semiempirical dissipation source functions for ocean waves. Part I: Definition, calibration, and validation. *Journal of Physical Oceanography* 40, 1917–1941.

Barber, N.F., Ursell, F., 1948. The generation and propagation of ocean waves and swell. I. Wave periods and velocities. *Philosophical transaction of the royal society. London* 240A, 527–560.

Bhowmick, A.S., Kumar, Raj, Chaudhuri, Sutapa, Sarkar, Abhijit, 2011. Swell propagation over Indian Ocean Region. *The International Journal of Ocean and Climate System* 2, 87–99.

DHI MIKE 21 Wave modelling user guide, 2009. DHI Water & Environment, Denmark, pp.13.

Hanson, J.L., Phillips, O.M., 1999. Wind sea growth and dissipation in the open ocean. *Journal of Physical Oceanography* 29, 1633–1648.

Hanson, J.L., Phillips, O.M., 2001. Automated analysis of ocean surface directional wave spectra. *Journal of Atmospheric and Oceanic Technology* 18, 277–293.

Janssen, P., 1998. On error growth in wave models vol 12. ECMWF Tech. Memo 249. European Centre for Medium-Range Weather Forecast, Reading, UK.

Janssen, P., 2000. ECMWF wave modeling and satellite altimeter wave data. In: Halpern, D (Ed.), *Satellite oceanography and society*. Elsevier, Amsterdam, pp. 35–56. Chap 3.

Kalantzi, G.D., Gommenginer, C., Srokosz, M., 2009. Assessing the performance of the dissipation parameterizations in WAVEWATCH III using collocated altimetry data. *Journal of Physical Oceanography* 39, 2800–2819.

Khandekar, M.L., 1989. *Operational Analysis and Prediction of Ocean Wind Waves*, Newyork. Spring Verlag., pp. 214.

Komen, G.J., Cavaleri, L., Donelan, M., Hasselmann, K., Hasselmann, S., Janssen, P.A.E.M., 1994. *Dynamics and Modeling of Ocean Waves*. Cambridge University Press.

Kumar, V.S., Anand, N.M., 2004. Variations in wave direction estimated using first and second order Fourier coefficients. *Ocean Engineering* 31, 2105–2119.

Kumar, V.S., 2006. Variation of wave directional spread parameters along the Indian coast. *Applied Ocean Research* 28, 98–103.

Munk, W.H., 1947. Tracking storms by forerunners of swell. *Journal of Meteorology* 4 (2), 45–57.

Parrish, D.E., Derber, J., Purser, J., Wu, W., Pu, Z., 1997. The NCEP global analysis system: Recent improvements and future plans. *Journal of Meteorological Society of Japan* 75, 18359–18365.

Pillar, P., Guedes, S.C., Carretero, J.C., 2008. 44-year wave hindcast for the North East Atlantic European coast. *Coastal Engineering* 55, 861–871.

Premkumar, K., Ravichandran, M., Kalsi, S.R., Sengupta, D., Gadgil, S., 2000. First results from a new observational system over the Indian Seas. *Current Science* 78, 323–330.

Rizvi, S.R.H., Rupa, K., Mohanty, U.C., 2000. Report on the utilization of MSMR data in the NCMRWF global data assimilation system. Report no. 1/2000. NCMRWF, New Delhi.

Senan, R., Anitha, D.S., Sengupta, D., 2001. Validation of SST and wind speed from TRMM using north Indian Ocean moored buoy observations. CAOS Report 200 1AS1, Centre for Atmospheric Sciences, Indian Institute of Science, Bangalore, India.

Sengupta, D., Goswami, B.N., Senan, R., 2001. Coherent intra-seasonal oscillations of ocean and atmosphere during Asian Summer monsoon. *Geophysical Research Letters* 28, 4127–4130.

Snodgrass, F.E., Groves, G.W., Hasselmann, K.F., Miller, G.R., Munk, W.H., Powers, W.M., 1966. Propagation of swell across the Pacific. *Philosophical Transaction of the Royal Society London* A259, 431–497.

Streeter, V.L., Wylie, E.B., Bedford, K.W., 1998. *Fluid Mechanics*. McGraw-Hill, Singapore.

Sudheesh K., Vethamony P., Babu M. T., JayaKumar S., 2004. Assessment of wave modeling results with buoy and altimeter deep water waves for a summer monsoon. Proceedings of the Third Indian National Conference on Harbour and Ocean Engineering (INCHOE—2004), NIO, Goa (India), 184–192.

Vethamony, P., Aboobacker, V.M., Menon, H.B., Ashok Kumar, K., Cavaleri, L., 2011. Superimposition of wind seas on pre-existing swells off Goa coast. *J. Mar. Syst* 87 (1), 47–54.

Vethamony, P., Sudheesh, K., Rupali, S.P., Babu, M.T., Jayakumar, S., Saran, A.K., Basu, S.K., Kumar, R., Sarkar, A., 2006. Wave modelling for the north Indian Ocean using MSMR analysed winds. *International Journal of Remote Sensing* 27 (18), 3767–3780.

Group, WISE, 2007. Wave modelling—the state of the art. *Progress in Oceanography* 75, 603–674.

Young, I.R., 1999. Wind generated ocean waves, in Elsevier Ocean Engineering book series vol. 2.